



Optical RF Phase Shifter Design Employing Optical Phase Manipulation and Coherent Detection – Part II: Numerical Demonstration

Linh V.T. Nguyen

Defence Science & Technology Organisation, Electronic Warfare & Radar Division
Edinburgh, South Australia 5111
E-mail: linh.nguyen@dsto.defence.gov.au

Abstract- An optical radio-frequency (RF) phase shifter concept employing optical phase manipulation of a double-sideband (DSB) modulated optical signal and coherent detection has been previously proposed in Part I. In this paper, an industry-standard photonic simulator is utilized to numerically demonstrate this optical RF phase shifter concept and investigate its performance. Linear phase responses are successfully demonstrated over a frequency range of 10-50 GHz. Various noise artifacts inherent in the design are identified. A number of design trade-offs are investigated and discussed. A possible feed-forward solution to suppress common-mode low-frequency noise and second-order harmonic artifacts is simulated.

Index Terms- RF photonics, microwave photonics, optical RF phase shifter, photonic microwave phase shifter, photonic signal processing, analogue signal processing.

I. INTRODUCTION

In the optical domain, the RF amplitude processing can be implemented with relative ease [1]. The ability to perform RF phase shifting through the manipulation of optical phase and coherent detection with electronic control signals has been identified as an attractive optical RF phase shifter concept suitable for complex optical RF signal processing [2].

In Part I [2], an optical RF phase shifter topology employing optical phase manipulation of a DSB modulated optical signal and coherent detection has been proposed. The technique performs broadband electrical phase shifting directly in the

optical domain. Its principles of operation as a standalone sub-system enable electrical phase shifting to be performed on the DSB modulated optical signal unrestrictedly at any location in an RF photonic network. Qualitative analysis has shown that the proposed optical RF phase shifter has low RF phase error and no output amplitude-phase interdependency [2].

In this paper, the results from the numerical analysis and demonstration of the proposed optical RF phase shifter [2] are presented. The proof-of-concept demonstration is performed by numerical simulations using VPItransmissionMaker™ photonic simulation software [3]. The report is structured as follows. Section 2 briefly reviews the design of the proposed optical RF phase shifter from [2]. Section 3 summarizes the simulated results and provides a discussion of the numerical proof-of-concept demonstration, while Section 4 presents the conclusion.

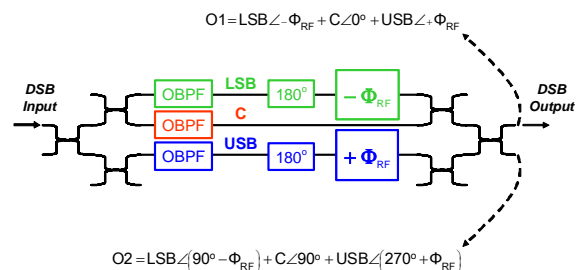


Fig. 1. Optical RF phase shifter topology [2].



II. PROPOSED TOPOLOGY

The proposed optical RF phase shifter topology is shown in Fig. 1 [2]. It utilizes optical integrated cross-couplers and bandpass filters. The lower sideband, carrier and upper sideband are first demultiplexed into individually components using integrated optical bandpass filters (OBPFs). Then the optical phase manipulation is performed [2]. The multiplexing function in Fig. 1 is achieved by using the optical cross-couplers to combine the filtered and phase-shifted optical signals. The intention of the topology depicted in Fig. 1 is to focus on the optical RF phase shifting function to simplify the scope of the concept demonstration.

III. NUMERICAL DEMONSTRATION

The VPItransmissionMaker™ [3] model of the proposed optical RF phase shifter is depicted in Fig. 2. Default parameters were used in all VPItransmissionMaker™ modules. The RF front-end consisted of a continuous-wave (CW) 100-mW laser diode, an ideal amplitude modulator having a modulation index of 0.5 and a sinusoidal signal synthesizer with output amplitude of 0.25 arbitrary units (a.u.). Coupling ratios were all 0.5. Three variable optical phase shifters were implemented in the VPItransmissionMaker™ model, as shown in

Fig. 2, so that the optical phase manipulation described by either (4) or (5) in [2] could be employed. A reference photonic link was also modeled to generate a reference signal. The RF back-end consisted of broadband PDs followed by direct-current (DC) blocks. An ideal electronic amplifier with 6-dB gain was used at the output of the optical RF phase shifter to equalize its AC amplitude with the reference photonic link. The modeling sample rate was chosen to be 640 GHz.

Initially, all OBPFs were set to have Gaussian passbands. The bandwidths of the OBPFs were set to 2 GHz and 10 GHz for the optical carrier and sidebands, respectively. The centre frequencies of sideband OBPFs were equally offset from the optical carrier by 20 GHz. The input RF signal frequency was simulated at 20 GHz. These settings were employed indicatively to quickly verify the functionality of the optical RF phase shifter model. Details on how these OBPF settings affect the RF phase shifting performance are to be augmented later on.

A. Elementary Simulated Results

Fig. 3 shows the optical and RF spectra of the reference photonic link. In comparison, Fig. 4 exhibits the optical and RF spectra of the optical RF phase shifter. The spectral characteristics of the RF signal recovered from the reference

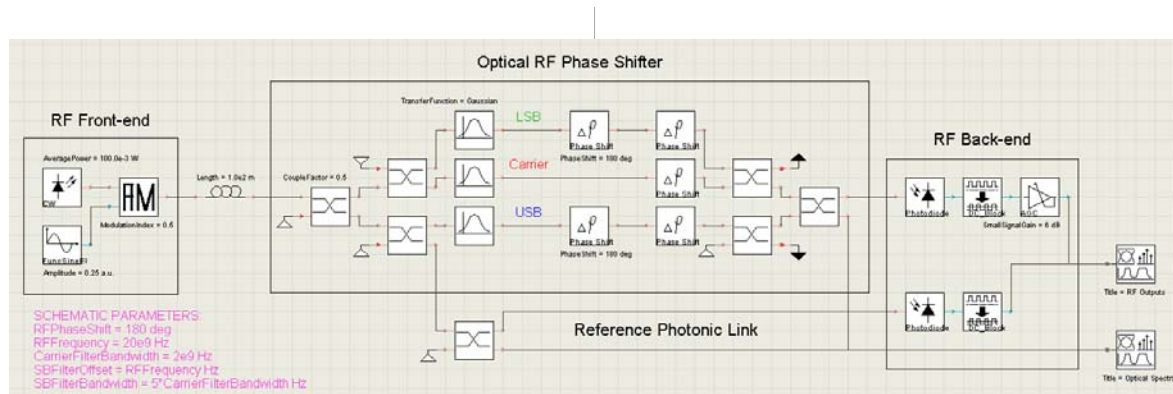


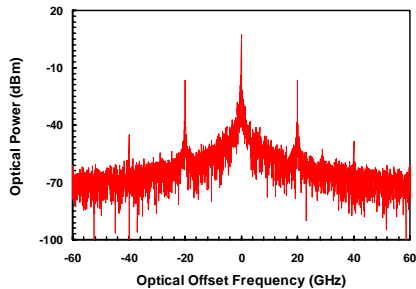
Fig. 2. The VPItransmissionMaker™ model of the proposed optical RF phase shifter topology.



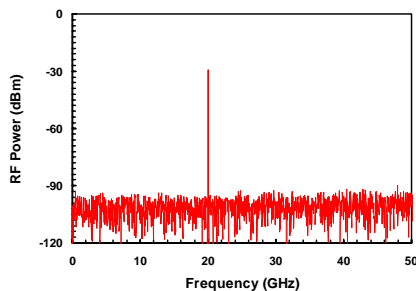
phonic link is clean as expected due to the high level of optical coherence [4]-[5]. In addition, its second-order harmonics are completely suppressed by a quadrature-biased amplitude modulator. Fig. 4 provides a qualitative performance in comparison to the photonic link in Fig. 3. Figures of merit such RF gain, dynamic range and sensitivity cannot be determined accurately from modeling without actual measured device characteristics.

From Fig. 4, the RF spectrum at output O1 (refer to Fig. 1) exhibits low-frequency noise and second-order harmonic artifacts. The second-order harmonic artifact is as expected [2], but the low-frequency noise artifact and its generation deserve further investigation. This noise artifact needs to be eliminated, because it lies in the likely intermediate-frequency bandwidth if the output is required to be down-converted for specialized digital signal processing.

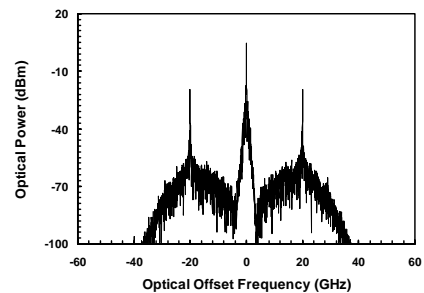
An interesting spectral artifact is observed on the RF spectra at output O2 (refer to Fig. 1) as shown in Fig. 4. There is no RF signal present at 20 GHz as expected [2]. There is an unexpected broadband noise artifact centered at 20 GHz whose distribution closely matches the sideband OBPF's transfer function, which also warrants further investigation.



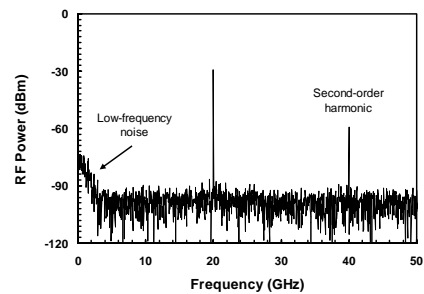
(a) Optical spectrum



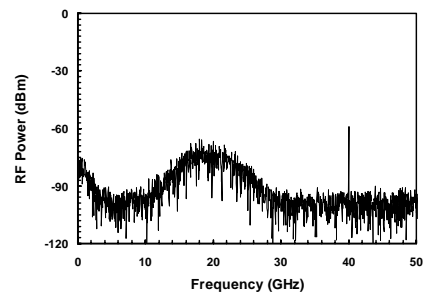
(b) RF spectrum



(a) Optical spectrum



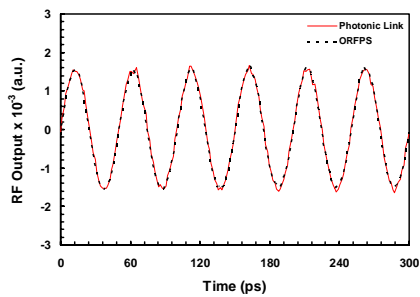
(b) RF spectrum at output O1



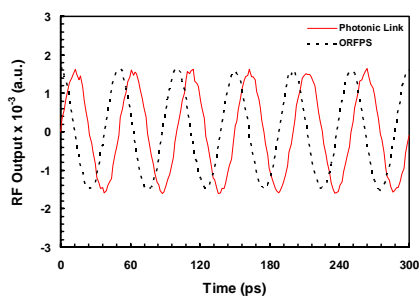
(c) RF spectrum at output O2

Fig. 3. Simulated optical and RF spectra of the photonic link at 20 GHz.

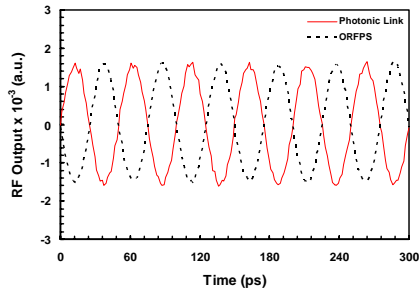
Fig. 4. Simulated outputs of optical RF phase shifter for zero-degree phase shift. The bandwidth of the sideband OBPFs was 10 GHz.



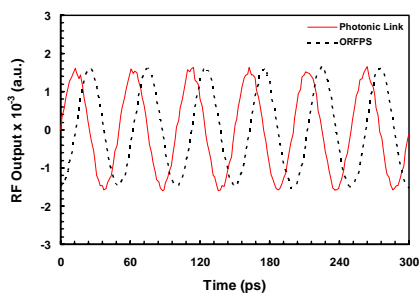
(a) Zero-degree phase shift



(b) 90-degree phase shift



(c) 180-degree phase shift



(d) 270-degree phase shift

Fig. 5. Simulated phase-shifted outputs from the optical RF phase shifter at 20 GHz. ORFPS, optical RF phase shifter.

It is evident from the simulations with VPItransmissionMaker™ that the proposed concept illustrated in Fig. 1 does function as the intended optical RF phase shifter. Examples of its phase-shifted RF signals at output O1 are depicted in Fig. 5 f or phase shifts of 0°, 90°, 180° and 270°. It is worth reiterating that these are true RF phase shifts performed in the optical domain.

B. Optical Filtering and Noise Artifacts

i. Common-Mode Low-Frequency Noise Artifact

The common-mode low-frequency noise artifact at both outputs O1 and O2 was determined by detailed simulations to be generated by the bandpass filtering of the optical carrier. Optical filtering of the lasing mode in laser diodes increases its partition noise [6]. In a singlemode laser diode, the generation of partition noise is between the lasing mode and spontaneous emission in a similar manner to competing longitudinal modes in multimode semiconductor lasers [6]-[7]. Consequently, this common-mode low-frequency noise artifact is expected to depend greatly on the OBPF that demultiplexes the optical carrier. Narrowband filtering of the optical carrier induces high level of partition noise, which potentially can become a dominating noise source. This was observed in simulations utilizing a carrier OBPF bandwidth of 0.5 GHz. The wider the OBPF, the more spontaneous emission is passed through with the optical carrier thereby reducing the partition noise. The carrier OBPF also restricts the low frequency limit of the optical RF phase shifter.

Simulations also illustrated how the type of OBPFs, e.g. Gaussian or rectangular transfer function, affected the common-mode low-frequency noise artifact. Gaussian OBPFs provide a gradual roll-off, while rectangular OBPFs induce a sharp cut-off at the expense of high noise power. Through detailed simulations, a carrier OBPF having a Gaussian transfer function with bandwidth of 2 GHz is a good compromise.



ii. Broadband Noise Artifact at Output O2

The broadband noise artifact observed at output O2 was confirmed to be due to the beat noise caused by the mixing between the optical carrier and spontaneous emission accompanying the sidebands. A detailed qualitative analysis is required to understand how this broadband noise artifact behaved differently at outputs O1 and O2. At the input, the DSB components generated by the EOM are in-phase with each other. However, the filtered spontaneous emission accompanying the lower sideband is out-of-phase with that accompanying the upper sideband. This is a characteristic of partition noise [8]-[9].

The vectorial representation of the DSB components together with the filtered spontaneous emission components propagating through the proposed optical RF phase shifter can be found in Fig. 6. While the sideband components mix with the optical carrier constructively at output O1, the beat noise generated by the mixing of the optical carrier and filtered spontaneous emission components is combined destructively. The contrary applies at output O2, hence the broadband noise artifact matching the sideband OBPF's transfer function observed at output O2 is a product resulted from the mixing of carrier and filtered spontaneous emission components.

Another design consideration is the symmetry of the transfer functions of both sideband OBPFs used in the proposed optical RF phase shifter. Perfect cancellation of the broadband noise artifact around the RF signal at output O1 was only possible because the sideband OBPFs were offset by the same amount from the optical carrier frequency and their transfer functions were the same. The lineshape of the laser model used was also symmetrical and Lorentzian. Simulation was performed with asymmetrical sideband OBPFs by setting the bandwidths in the lower and upper sideband paths to 10 GHz and 6 GHz, respectively. The simulated optical and RF spectra from output O1 are plotted in Fig. 7. In this case, it is evident that the cancellation of the

beat noise caused by the optical carrier and the spontaneous emission accompanying the sidebands is imperfect. It therefore highlights the need for the sideband OBPFs to be designed and matched as close to each other as possible to maximize the cancellation of the beat noise generated by the mixing of the optical carrier and filtered spontaneous emission components. These sideband OBPFs cannot however be made narrowband since that would defeat the preferred advantages and purpose of performing analogue signal processing in the optical domain.

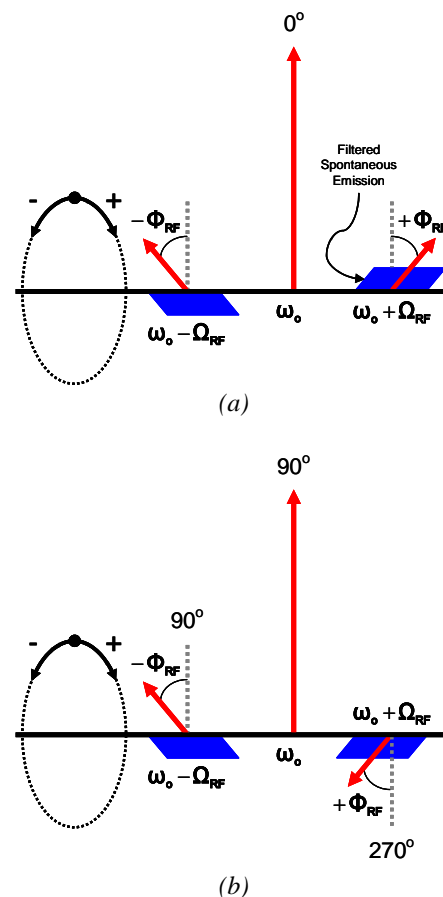


Fig. 6. Vectorial representation of the DSB modulated optical signal and filtered spontaneous emission through the proposed optical RF phase shifter at outputs (a) O1, and (b) O2. Clockwise direction is chosen for positive phase.

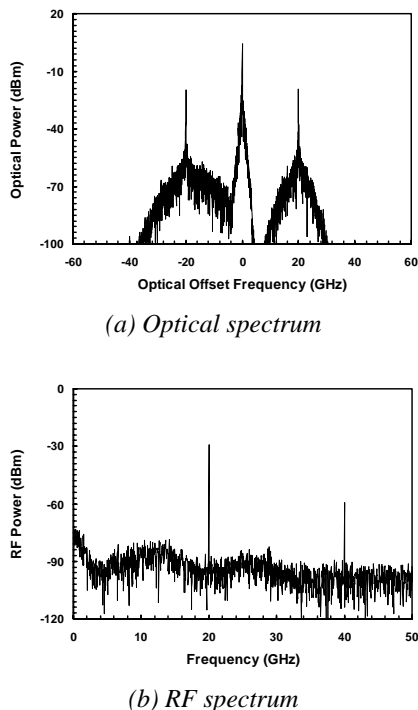


Fig. 7. Simulated optical and RF spectra at output O1 of the optical RF phase shifter having asymmetrical sideband Gaussian OBPFs. Zero-degree phase shift was used.

iii. Effect of Filter Crosstalk

It is evident from the analysis and simulations presented so far that the optical RF phase shifters require the input DSB optical signal to be demultiplexed and filtered with sharp roll-off passbands into the individual components prior to the optical phase manipulation. This is particularly important for low signal frequencies when the sidebands are close to the carrier. In the optical RF phase shifter topology presented in Fig. 1, there is potential for optical carrier leakage through to the sideband paths, and vice versa. Its performance is dependent on the sharpness of the roll-offs of the OBPFs. Signal leakage at the OBPFs will result in in-band interference at the output PD since optical cross-couplers are broadband devices. For example, any optical carrier leakage occurring in the

sideband paths will interfere with that from the carrier path in a complex vectorially manner, i.e. amplitude and phase. A similar argument is applicable for sideband leakage through the carrier path. The outcome can either be an increase or decrease in the detected RF power depending on the resultant complex optical interference.

C. Feed-Forward Cancellation of Unwanted Artifacts

It has been shown in Fig. 4 that output O2 also contains both common-mode low-frequency noise and second-order harmonic artifacts similar to output O1. A feed-forward scheme to suppress both the common-mode low-frequency noise and second-order harmonic artifacts will be conceptually tested.

The low-frequency noise artifact was determined to be a common-mode feature at both outputs O1 and O2. If output O2 is detected with a PD and then low-pass filtered, it can be subtracted from output O1 to suppress the common-mode low-frequency noise artifact. This is a technique often used in coherent optical receiver design [10]. The electrical low-pass filter (LPF) can be a simple Gaussian type with a bandwidth set to the same value as the bandwidth of the carrier OBPF. This LPF must not pick up any of the broadband noise artifact at output O2. Any residual broadband noise artifact will be undesirably added to output O1.

It can be easily demonstrated through analysis that the second-order harmonic artifact from output O2 is *always* out-of-phase in comparison to that being produced at output O1. If output O2 is once again detected with a PD and its second-order harmonic artifact extracted, then it can be added to that of output O1 to cancel out the second-order harmonic artifact. The second-order harmonic artifact from output O2 can be extracted by using a tracking electrical bandpass filter (BPF), whose bandwidth can be set indicatively at 1 GHz. Once again, the transfer function of the BPF can be a simple Gaussian



type. In this scheme, any residual broadband noise artifact at output O2 passing through the tracking BPF will be added to output O1. The VPItransmissionMaker™ implementation of a feed-forward compensated receiver suitable for suppressing both common-mode low-frequency noise and second-order harmonic artifacts in the proposed optical RF phase shifter is exhibited in Fig. 8.

D. Complete Design and Broadband Demonstration

The proposed optical RF phase shifter has only been so far numerically demonstrated in a narrowband mode. The main reason is to build a foundation to understand its various design and performance issues. With that done, the complete design for the broadband optical RF phase shifter concept can now be discussed and demonstrated.

It is evident from earlier simulation results that a suitable carrier OBPF in the optical RF phase shifter has a bandwidth of 2 GHz and Gaussian transfer function. The bandwidth of the LPF in the feed-forward compensated receiver is consequentially set at 2 GHz. Unlike the carrier OBPF, the sideband OBPFs are broadband and have flat-top passbands. For broadband RF phase shifting operation, the sideband OBPFs are

required to have bandwidths of at least 40 GHz, which are modeled with trapezoidal transfer functions. The stop-bands of the trapezoidal OBPFs are conservatively set at 50 GHz and 40 dB down from peak transmission. The centre frequencies of these sideband OBPFs are set at an offset of 30 GHz from the optical carrier keeping the crosstalk between adjacent carrier and sideband OBPFs at a manageable level. These parameters set up a simulated optical RF phase shifter with an operating frequency range of 10-50 GHz. Operation below 10 GHz and above 50 GHz will of course require selection of alternative combinations of OBPFs. The feed-forward compensated receiver shown in Fig. 8 is also utilized in the complete broadband design of the proposed optical RF phase shifter.

Fig. 9 summarizes simulation results from the broadband optical RF phase shifter model from 10 to 50 GHz. The RF phase shift was arbitrarily chosen to be 90°. The nature of broadband characteristics is only limited by the bandwidth of the sideband OBPFs utilized in the modeled design. The output AC amplitudes are constant for all signal frequencies, as alluded to in the theoretical analysis presented in [2], highlighting the low amplitude-phase interdependency.

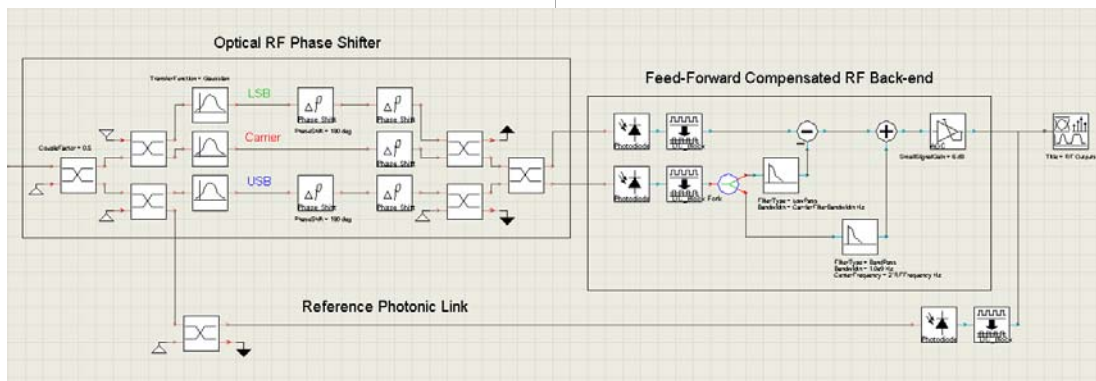
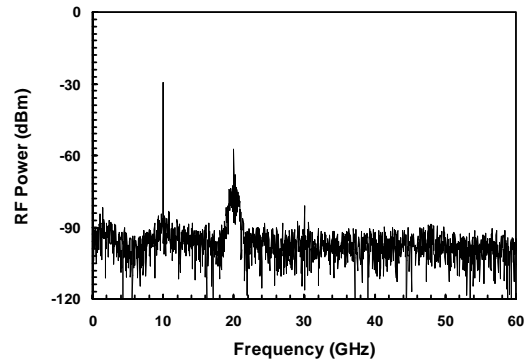
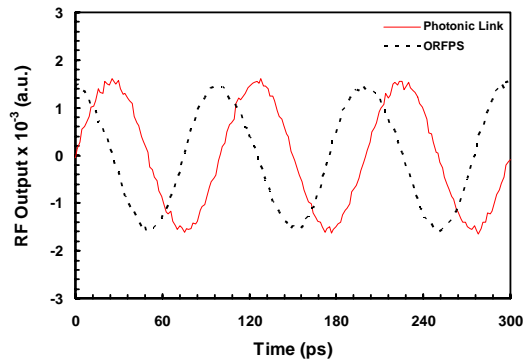
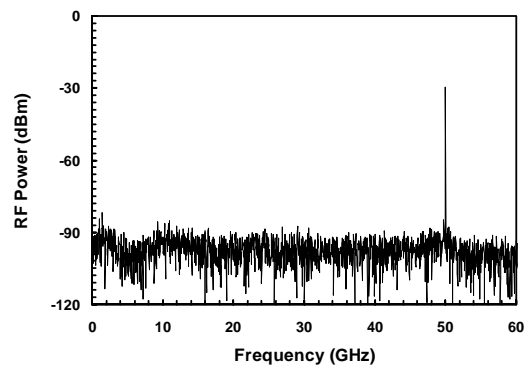
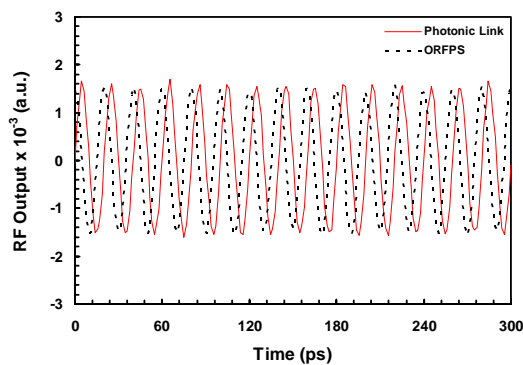


Fig. 8. VPItransmissionMaker™ model of a feed-forward compensated receiver to suppress both low-frequency noise and second-order harmonic artefacts in the proposed optical RF phase shifter.



(a) Temporal and spectral outputs for 10 GHz



(b) Temporal and spectral outputs for 50 GHz

Fig. 9. Simulated temporal and spectral outputs of the broadband optical RF phase shifter at 90 degrees. ORFPS, optical RF phase shifter.

Two observations can be made from the simulated results shown in Fig. 9. Firstly, the common-mode low-frequency noise artifact due to optical carrier partition noise is successfully suppressed utilizing a feed-forward compensation scheme. The choices for various OBPFs and electrical LPF are sound. Secondly, the second-order harmonic artifact cannot be suppressed. The tracking BPF in the receiver picks up the broadband noise artifact at output O2 within its bandwidth, which is then added to output O1. It can be satisfactorily concluded that the feed-forward cancellation of the second-order harmonic artifact is ineffective in a broadband optical RF phase shifter design. The management of the second-order harmonic

artifact is recommended to be achieved by the application of suitable output PDs as previously discussed in [2].

E. Further Discussion

A series of simulations similar to those in Fig. 9 were performed as a function of signal frequency. The simulated outputs from the modeled optical RF phase shifter and reference photonic link were written to a file and compared utilizing a simple LabVIEW™ algorithm to extract the phase difference. Various RF phase shifts including 0, 20, 40, 80, 90, 120, 150, 180, 200, 225, 250, 270, 285, 300, 315, 330 and 345 degrees were modeled.

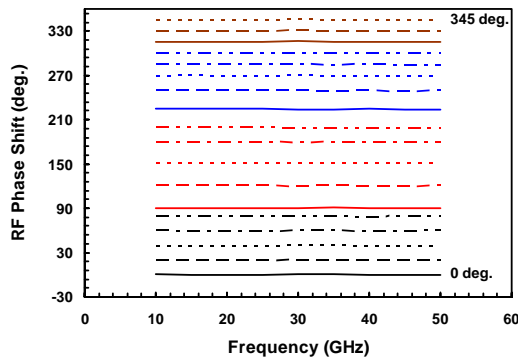


Fig. 10. Simulated RF phase shifting ranging from 0 to 345 degrees from the proposed optical RF phase shifter as a function of signal frequency.

The overall result is plotted in Fig. 10, whose lines depict the phase shifts being modeled. At 360 degrees, the output is exactly the same as at zero phase shift. Fig. 10 shows in principle that the proposed optical RF phase shifter is highly linear and there is extremely low amplitude-phase interdependency, which is a highly desirable characteristic for all RF phase shifter.

The simulation scenario from Fig. 9 was repeated at 40 GHz and having the offset of the sideband OBPFs from the optical carrier adjusted from 30 GHz to 25 GHz. The simulated RF spectrum is depicted in Fig. 11. The distribution of the broadband noise artifact generated at output O2 in this case extends to near DC. The near-DC component is passed through the electrical LPF in the feed-forward compensated receiver and added to output O1 rendering the feed-forward noise suppression scheme ineffective. The interaction between optical filtering and electrical noise generation is therefore an important consideration when designing a broadband optical RF phase shifter with a feed-forward noise suppression scheme.

The architecture of the optical RF phase shifter investigated in this report lends itself to be implemented in photonic integrated circuitry. The material of choice to implement the optical

RF phase shifter must have ultralow dependence of the refractive index on wavelength for electro-optic phase modulation. It must also be ideally immune to the operating environment to ensure that coherent detection.

The most anticipated technical challenge would be the planar OBPFs, since optical cross-couplers and phase shifters can be readily fabricated. The OBPF for the carrier path suffices to be Gaussian and narrowband, while the OBPFs for the sideband paths need to be broadband with flat-top passband transfer functions and have sharp response cut-offs. At the same time, the OBPFs for the sidebands must have mirror-image responses relative to the optical carrier. This is a very stringent technical challenge. Nevertheless, it is hoped that the development of photonic integrated circuitry will be able to address this technical challenge in the near future.

Tuneability of the centre frequencies of all OBPFs in the optical RF phase shifter architecture must be utilized as a quality control parameter to ensure that its performance can be optimized. A variable optical attenuator can be incorporated after the OBPF of carrier path to provide additional output RF amplitude control, according to (3) to (6) in [2]. This will further enhance the versatility and practicality of the optical RF phase shifter design outlined in [2] and investigated in this report.

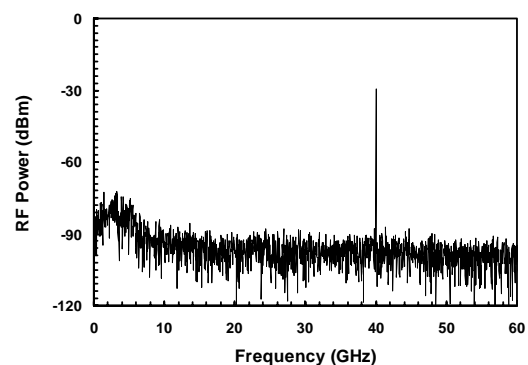


Fig. 11. Noise cancellation became ineffective with unsuitable choices of optical and electrical filters.



In this report, only static performance has been investigated. Since the proposed optical RF phase shifter topology presented in this report utilizes electro-optic phase manipulation, it is envisaged that high-speed modulation of the RF phase would be possible as a direct result of the high-speed optical phase modulation. The dynamic performance of this optical RF phase shifter would be a topic of a future study.

IV. CONCLUSION

In this paper, the optical RF phase shifting concept employing optical phase manipulation and coherent detection has been numerically demonstrated utilizing VPItransmissionMaker™. This enabled a rigorous and thorough investigation to be carried out. Firstly, the partition noise of the filtered optical carrier produces the common-mode low-frequency noise artifact. Through proper design, the suppression of this noise is possible utilizing a feed-forward scheme. Secondly, the beat noise caused by the mixing between the optical carrier and spontaneous emission accompanying the sidebands is broadband. In order to minimize this beat noise, the OBPFs in the sideband paths must have their transfer functions symmetrically matching each other. The numerical demonstration was concluded with the simulation of a broadband optical RF phase shifter design capable of achieving linear RF phase shifts for the frequency range of 10-50 GHz. However, the feed-forward cancellation of second-order harmonic artifact is ineffective.

In conclusion, this optical RF phase shifter concept has the potential to be very useful for developing analogue RF photonic systems. If successfully implemented, such an optical RF phase shifter would have wide ranging applications for analogue RF photonic signal processing including optically-fed phased-array antennas, optical RF filtering, and frequency translation in defence systems to name a few.

ACKNOWLEDGMENT

The author would like to thank Associate Professor Arnan Mitchell and Dr. Lam Bui of RMIT University, Australia, for useful discussions, and Mr. Daniel Borg of the Defence Science & Technology Organisation, Australia, for post-simulation signal processing.

REFERENCES

- [1] R.A.Minasian, "Photonic signal processing of microwave signals", *IEEE Trans Microw. Theory Tech.*, Vol. 54, pp. 832-846, February 2006
- [2] L.V.T.Nguyen, "Optical RF Phase Shifter Design Employing Optical Phase Manipulation and Coherent Detection - Part I: Concept Proposal", *Int. J. Microw. Opt. Technol.*, Vol.6.No.5, pp.301-309, September 2011.
- [3] VPItransmissionMaker™ Cable Access Software (Version 7.6). Company website at <http://www.vpisisystem.com>
- [4] X.Luo, X.Han, Y.Gu, S.Li and M. Zhao, "Phase noise characteristics of the carrier transmitted by the double-sideband-carrier-suppressed modulation system", *Opt. Engineering*, Vol. 48, pp. 105007-1-5, October 2009
- [5] G.Qi, J.Yao, J.Seregelyi, S.Paquet and C.Bélisle, "Generation and distribution of a wide-band and continuously tunable millimeter-wave signal with an optical external modulation technique", *IEEE Trans Microw. Theory Tech.*, Vol. 53, pp. 3090-3097, October 2005
- [6] D.Cutrer, P.Pepeljugoski and K.Lau, "Noise properties of electrically gain-switched 1.5 μ m DFB lasers after spectral filtering", *Electron. Letts.*, Vol. 30, pp. 1418-1419, August 1994
- [7] S.Yamamoto, H.Sakaguchi and N.Seki, "Measurement of mode partition in DFB lasers", *J. Lightw. Technol.*, Vol. 4, pp. 672-679, June 1986
- [8] S.Pradhan, G.E.Town and K.J. Grant, "Dual-wavelength DBR fiber laser", *IEEE Photon. Technol. Letts.*, Vol. 18, pp. 1741-1743, August 2006
- [9] S.Pradhan, G.E.Town and K.J. Grant, "Multiwavelength distributed Bragg reflector fiber laser", *Electron. Letts.*, Vol. 42, pp. 963-964, August 2006
- [10] S.Yamashita and T.Okoshi, "Suppression of beat noise from optical amplifiers using coherent receivers", *J. Lightw. Technol.*, Vol. 12, pp. 1029-1035, June 1994